

Protecting geometric quantum discord via partially collapsing measurements of two qubits in multiple bosonic reservoirs

Xue-Yun Bai(白雪云) and Su-Ying Zhang(张素英)

Citation: Chin. Phys. B, 2022, 31 (**4**): 040308. DOI: 10.1088/1674-1056/ac4f54
Journal homepage: http://cpb.iphy.ac.cn; http://iopscience.iop.org/cpb

What follows is a list of articles you may be interested in

Quantum properties near the instability boundary in optomechanical system

Han-Hao Fang(方晗昊), Zhi-Jiao Deng(邓志姣), Zhigang Zhu(朱志刚), and Yan-Li Zhou(周艳丽)
Chin. Phys. B, 2022, 31 (**3**): 030308. DOI: 10.1088/1674-1056/ac40f7

Tetrapartite entanglement measures of generalized GHZ state in the noninertial frames

Qian Dong(董茜), R. Santana Carrillo, Guo-Hua Sun(孙国华), and Shi-Hai Dong(董世海)
Chin. Phys. B, 2022, 31 (**3**): 030303. DOI: 10.1088/1674-1056/ac2299

Probabilistic resumable quantum teleportation in high dimensions

Xiang Chen(陈想), Jin-Hua Zhang(张晋华), and Fu-Lin Zhang(张福林)
Chin. Phys. B, 2022, 31 (**3**): 030302. DOI: 10.1088/1674-1056/ac1efb

Quantum multicast communication over the butterfly network

Xing-Bo Pan(潘兴博), Xiu-Bo Chen(陈秀波), Gang Xu(徐刚), Zhao Dou(窦钊), Zong-Peng Li(李宗鹏), and Yi-Xian Yang(杨义先)
Chin. Phys. B, 2022, 31 (**1**): 010305. DOI: 10.1088/1674-1056/ac20c6

Geometric quantum discord and Berry phase between two charge qubits coupled by a quantum transmission line

Zhu Han-Jie, Zhang Guo-Feng
Chin. Phys. B, 2014, 23 (**12**): 120306. DOI: 10.1088/1674-1056/23/12/120306

Protecting geometric quantum discord via partially collapsing measurements of two qubits in multiple bosonic reservoirs

Xue-Yun Bai(白雪云) and Su-Ying Zhang(张素英)†

Institute of Theoretical Physics and State Key Laboratory of Quantum Optics and Quantum Optics Devices, Shanxi University, Taiyuan 030006, *China*

(Received 28 December 2021; revised manuscript received 25 January 2022; accepted manuscript online 27 January 2022)

We study the dynamics of geometric quantum discord (GQD) between two qubits, each qubit interacting at the same time with K independent multiple bosonic reservoirs at zero temperature. In both weak and strong qubit–reservoirs coupling regimes, we find that the increase of the number K of reservoirs can induce the damped oscillation of GQD, and enhance the memory effects of the overall environment. And the Hilbert–Schmidt norm GQD (two-norm GQD) is always smaller than the trace norm geometric quantum discord (one-norm GQD). Therefore, the one-norm GQD is a better way to measure the quantum correlation. Finally, we propose an effective strategy to improve GQD by using partially collapsing measurements, and we find that the protection effect is better with the increase of the weak measurement strength.

Keywords: geometric quantum discord (GQD), the Hilbert–Schmidt norm GQD, the trace norm GQD, partially collapsing measurements

PACS: 03.65.Ud, 03.65.Ta **DOI:** 10.1088/1674-1056/ac4f54

1. Introduction

Quantum entanglement, the most common measure of quantum correlations, plays a vital role in the field of quantum information processing. For instance, it is widely used in the quantum computation,[1–4] quantum teleportation,[5] and quantum cryptography.[6] For many years, entanglement was considered as the only type of quantum correlations useful for quantum technology. However, it is gradually recognized that entanglement is not completely equivalent to quantum correlation, and some unentangled quantum states can still complete some quantum information processing tasks.[7] To characterize and quantify all of the nonclassical correlation contained in a given quantum state, quantum discord (QD)[8] as a new and the most popular correlation measurement has come into our view, which is defined as the difference between the total correlation and the locally accessible classical correlation. It has been shown that QD can be nonzero for some separable mixed states[9,10] and could be viewed as an invaluable resource of quantum computation and quantum communication. At present, QD has become a hot topic of special attention in the international academia, and many related theories[11–13] and experimental works[14–16] have emerged.

The QD plays a very important role in quantum computation,[17] local broadcasting,[18] remote state preparation,[19] thermodynamics of information,[20] quantum many-body systems,[21] and so on. However, only some special two-qubit states can obtain the exact analytical expression of QD, and the exact expression of QD for an arbitrary state of two qubits is unattainable.[22,23] So various types of alternative discord-like correlation quantifiers were introduced subsequently,[24,25] such as measurement-induced nonlocality (MIN),[26] geometric quantum discord (GQD),[27] measurement-induced disturbance (MID)[28] and global quantum discord,[29] etc. In 2010, Dakic *et al.* proposed the geometric quantum discord based on Hilbert–Schmidt norm (two-norm GQD),[27] and derived an explicit formula for measuring any two qubits. Although the two-norm GQD offers the advantage of easier computability, in view of two-norm GQD will increase the unmeasured part under the specific local operation, it is not the best way to measure the quantum correlation.[30–32] In order to avoid this problem, Paula *et al.* proposed the geometric quantum discord based on trace norm (one-norm GQD)[33] in 2013, which can completely solve the problems of two-norm GQD.

Due to the ubiquitous environment, any quantum system is difficult to exist in isolation. It is of practical significance to analyze the QD behavior in open systems. Up to now, some achievements have been made in this respect.[34–48] For instance, Mohamed *et al.*[34] showed that there is no asymptotic decay for MIN while asymptotic decay exists for GQD, and the evolvement periods of GQD and MIN get shorter with the increase in the dipole–dipole interaction parameter, for a two-atom system in the non-degenerate two-photon Tavis–Cummings model. For the single sided and two-sided noisy channels,[35] even when the qubits are initially prepared in some mixed states, measurement-induced nonlocality can be expressed as the product of the initial measurement induced nonlocality and the channels' action on the maximally entangled state. However, for the measurement-induced disturbance and quantum discord, there is no similar factorization

†Corresponding author. E-mail: zhangsy@sxu.edu.cn

© 2022 Chinese Physical Society and IOP Publishing Ltd

law. Reference [37] illustrated that different initial states can be distinguished by using GQD, and the depolarizing channels heavily influence the dynamics of GQD and MIN as compared to the amplitude damping channel. Furthermore, no GQD and MIN sudden death is seen at finite temperature even in the presence of decoherence. Kenfack *et al.*[43] unveiled that the immunity of entanglement and QD against decoherence can be efficiently increased by properly adjusting the parameters of the input states, no matter the spectrum of the colored noise and the number of random bistable fluctuator (RBF) considered, and QD can be completely shielded from the decoherence by performing a weak measurement followed by its weak measurement reversal on the qubit of the system even when the decoherence process is strengthen with a large number of RBF affecting the qutrit. In the fidelity of teleportation and QD, the channel state are more stable and most efficiently under the influence of a dephasing environment than those under the influence of a dissipative or noisy environment.[47]

As is well known, the dynamics of a two-level open system weakly coupled to a single environment only exhibits Markovian behavior. However, it shows non-Markovian behavior even in the weak-coupling regimes if the system is coupled simultaneously to many environments. The consideration of simultaneous affections of multiple environments on a open system is relevant in many realistic situations, so it is necessary to understand the quantum dynamics problems in complex environment.[49–51] The geometric quantum discord dynamics of two-qubit states in this complex environment has not been studied so far. In this paper, based on the two-qubit systems interacting with their respective K independent reservoirs of field modes, we discuss the effects of the qubit–reservoir coupling and the number of reservoirs on two-norm GQD and one-norm GQD, and some meaningful conclusions are obtained.

The paper is structured as follows. We introduce the criterion for achieving the GQD of the Hilbert–Schmidt norm and the trace norm in Section 2. In Section 3, we give the model based on a two-level atom simultaneously interacting with K independent reservoirs. Time evolution of two-norm GQD and one-norm GQD are investigated in Section 4. In Section 5, we investigate the protection of the GQD for entangled two-qubit systems by applying partially collapsing measurement. Finally, we conclude our work in Section 6.

2. Preliminaries

(A) The Hilbert–Schmidt norm geometric quantum discord (two-norm GQD). For a two-qubit system ρ^{AB}, two-norm GQD is defined as the minimal Hilbert–Schmidt distance between a state and the set of classical states,[27] namely,

$$D^2(t) = 2\min_{\rho_0\in R_0}\left\|\rho^{\mathrm{AB}}-\rho_0\right\|^2, \tag{1}$$

where we add a normalization factor 2, and $\|\chi\| = \sqrt{\mathrm{Tr}\left[\chi^{\dagger}\chi\right]}$ ($\chi = \rho^{\mathrm{AB}} - \rho_0$) denotes the norm in the Hilbert–Schmidt space. R_0 is the set of zero-discord states with the general form given by

$$\rho_0 = \sum_d p_d R_d^{\mathrm{A}} \otimes \rho_d^{\mathrm{B}}, \tag{2}$$

where $\{R_d\}$ denotes a set of orthogonal projectors for subsystem A with probability p_d ($\sum_d p_d = 1$) and ρ_d^{B} is a general reduced density operator for subsystem B.

According to the generalized Bloch representation of the density matrix, the state of an arbitrary two-qubit system can be written as[27]

$$\rho^{\mathrm{AB}}(t) = \frac{1}{4}\Bigg(I^{\mathrm{A}}\otimes I^{\mathrm{B}} + \sum_{i=1}^{3} x_i\sigma_i^{\mathrm{A}}\otimes I^{\mathrm{B}} + \sum_{i=1}^{3} I^{\mathrm{A}}\otimes y_i\sigma_i^{\mathrm{B}} + \sum_{i,j=1}^{3} t_{ij}\sigma_i^{\mathrm{A}}\otimes\sigma_j^{\mathrm{B}}\Bigg), \tag{3}$$

where $x_i = \mathrm{Tr}(\rho\sigma_i^{\mathrm{A}}\otimes I^{\mathrm{B}})$ and $y_i = \mathrm{Tr}(\rho I^{\mathrm{A}}\otimes\sigma_i^{\mathrm{B}})$ are components of the local Bloch vectors, $t_{ij} = \mathrm{Tr}(\rho\sigma_i^{\mathrm{A}}\otimes\sigma_j^{\mathrm{B}})$ denotes the correlation tensor with $\sigma_i^{\mathrm{A(B)}}$ being Pauli matrices.

The dynamic evolutions of the two-norm GQD comes out to be[27]

$$D^2(t) = \frac{1}{2}\left(\|X\|^2 + \|T\|^2 - \Omega_{\max}\right), \tag{4}$$

where $\Omega_{\max}$ is the largest eigenvalue of the matrix $\Omega = XX^{\mathrm{t}} + TT^{\mathrm{t}}$, whose elements are calculated from the column vector $X = (x_1, x_1, x_1)^{\mathrm{t}}$ and the correlation matrix $T = (t_{ij})$.

For the two-qubit states $\rho^{\mathrm{AB}}(t)$ with the X-shaped matrix form, two-norm GQD can be evaluated explicitly as[52]

$$D^2\left(\rho^{\mathrm{AB}}\right) = \frac{1}{2}\left(\alpha_1+\alpha_2+\alpha_3-\max\{\alpha_1,\alpha_2,\alpha_3\}\right), \tag{5}$$

where

$$\begin{aligned}\alpha_1 &= 4\left(|\rho_{14}|+|\rho_{23}|\right)^2,\\ \alpha_2 &= 4\left(|\rho_{14}|-|\rho_{23}|\right)^2,\\ \alpha_3 &= 2\left[\left(\rho_{11}+\rho_{33}\right)^2+\left(\rho_{22}+\rho_{44}\right)^2\right].\end{aligned}$$

(B) The trace norm geometric quantum discord (one-norm GQD). Similar with two-norm GQD, the one-norm GQD can be defined as[53–55]

$$D^1(t) = \min_{\rho_0\in R_0}\left\|\rho^{\mathrm{AB}}-\rho_0\right\|_1, \tag{6}$$

where $\|F\|_1 = \mathrm{Tr}\left[\sqrt{F^{\dagger}F}\right]$ ($F = \rho^{\mathrm{AB}} - \rho_0$) is the one norm and R_0 is the set of an arbitrary classical quantum state. For the X-form states, one-norm GQD can be obtained analytically

$$D^1\left(\rho^{\mathrm{AB}}\right) = \sqrt{\frac{\beta_1^2\beta_{\max}-\beta_2^2\beta_{\min}}{\beta_{\max}-\beta_{\min}+\beta_1^2-\beta_2^2}}, \tag{7}$$

where $\beta_{1,2}=2\left(|\rho_{14}|\pm|\rho_{23}|\right)$, $\beta_3=1-2\left(\rho_{22}+\rho_{33}\right)$, $\beta_{\max}=\max\left\{\beta_3^2,\beta_2^2+\beta_4^2\right\}$, and $\beta_{\min}=\min\left\{\beta_1^2,\beta_2^2\right\}$ with $\beta_4=2\left(\rho_{11}+\rho_{22}\right)-1$.

The value of $D^1(t)$ is confined in the range $0\le D^1(t)\le 1$, where the lower bound 0 indicates ρ^{AB} being a classical quantum state and the upper bound 1 means the maximum quantum correlation.

3. Physical model and basic concepts

In this section, let us for concreteness consider a two-level atom with ground state $|0\rangle$ and excited state $|1\rangle$ simultaneously interacting with K independent reservoirs of field modes. We assume all reservoirs initially in the vacuum and independent with each other. The Hamiltonian for the total system can be written as (with $\hbar=1$)[56]

$$H=H_0+H_{\mathrm{I}}, \tag{8}$$

with

$$H_0=\frac{\omega_0}{2}\sigma_z+\sum_{i=1}^{K}\sum_j\omega_{i,j}a_{i,j}^{\dagger}a_{i,j},$$
$$H_{\mathrm{I}}=\sum_{i=1}^{K}\sum_j g_{i,j}\left(\sigma_-a_{i,j}^{\dagger}+\sigma_+a_{i,j}\right),$$

where H_0 consists of the free Hamiltonian of atom and reservoirs, σ_z means a Pauli operator for the atom with transition frequency ω_0, and $a_{i,j}$ ($a_{i,j}^{\dagger}$) is the annihilation (creation) operator of field mode j with frequency $\omega_{i,j}$ in reservoir i. Besides, H_{I} is the interaction Hamiltonian of qubit and reservoirs. Concretely, $\sigma_{\pm}$ denotes the raising and lowering operators of the qubit, and $g_{i,j}$ denotes the coupling between the qubit and mode j in the i-th reservoir.

Here, we first suppose that the initial state of the qubit is of the form

$$|\psi(0)\rangle_{\mathrm{s}}=c_{\mathrm{e}}(0)|e\rangle_{\mathrm{s}}+c_{\mathrm{g}}(0)|g\rangle_{\mathrm{s}}, \tag{9}$$

and the state of K vacuum reservoirs reads $\prod_{i=1}^{K}|\bar{0}\rangle_i$ with $|\bar{0}\rangle_i=\prod_{j=1}|0_j\rangle_i$. Since there exists at most one excitation in the total system at any time, the initial state $|\Psi(0)\rangle=|\psi(0)\rangle_{\mathrm{s}}\otimes\prod_{i=1}^{K}|\bar{0}\rangle_i$ evolves after time $t>0$ into the state

$$|\Psi(t)\rangle=\left[c_{\mathrm{e}}(t)|e\rangle_{\mathrm{s}}+c_{\mathrm{g}}(0)|g\rangle_{\mathrm{s}}\right]\otimes\prod_{i=1}^{K}|\bar{0}\rangle_i$$
$$+|g\rangle_{\mathrm{s}}\otimes\sum_{i=1}^{K}\sum_j c_{i,j}(t)|1_j\rangle_i, \tag{10}$$

where $|1_j\rangle_i$ denotes that only the j-th mode of the bath in reservoir i is excited. Note that the amplitude $c_{\mathrm{g}}(0)$ is constant under the rotating wave approximation, while $c_{\mathrm{e}}(t)$ and $c_{i,j}(t)$ are time dependent.

To give the dynamics of these amplitudes in the interaction picture, we use the Schröinger equation. Then we can obtain the following differential equations:

$$\dot{C}_{\mathrm{e}}(t)=-\mathrm{i}\sum_{i=1}^{K}\sum_j g_{i,j}\mathrm{e}^{\mathrm{i}\left(\omega_0-\omega_{i,j}\right)t}C_{i,j}(t), \tag{11}$$

$$\dot{C}_{i,j}(t)=-\mathrm{i}g_{i,j}^{*}\mathrm{e}^{-\mathrm{i}\left(\omega_0-\omega_{i,j}\right)t}C_{\mathrm{e}}(t), \tag{12}$$

where $C_{\mathrm{e}}(t)=c_{\mathrm{e}}(t)\exp(\mathrm{i}\omega_0 t)$, and $C_{i,j}(t)=c_{i,j}(t)\exp(\mathrm{i}\omega_{i,j}t)$. Integrating Eq. (11) with the initial condition $C_{i,j}(0)=c_{i,j}(0)=0$, and substituting the result into Eq. (12), we can get a closed equation for $C_{\mathrm{e}}(t)$, namely,

$$\dot{C}_{\mathrm{e}}(t)=-\int_0^t \mathrm{d}t_1F(t-t_1)C_{\mathrm{e}}(t_1), \tag{13}$$

with the memeroy kernel $F(t-t_1)\equiv\sum_{i=1}^{K}f_i(t-t_1)$. The kernel $f_i(t-t_1)=\sum_j\left|g_{i,j}\right|^2\mathrm{e}^{\mathrm{i}\left(\omega_0-\omega_{i,j}\right)(t-t_1)}$ is a correlation function $f_i(t-t_1)$ of the ith reservoir, which in the limit of a large number of modes can be changed to an integration in terms of the spectral density $J_i(\omega)$ as

$$f_i(t-t_1)=\int_0^t \mathrm{d}\omega J_i(\omega)\exp[\mathrm{i}\left(\omega_0-\omega\right)(t-t_1)]. \tag{14}$$

By virtue of the linearity we note that the memeroy kernel $F(t-t_1)$ can be expressed as a Fourier transform of $\boldsymbol{J}(\omega)=\sum_{i=1}^{K}J_i(\omega)$, which can be obtained as

$$F(t-t_1)=\int_0^t \mathrm{d}\omega\boldsymbol{J}(\omega)\exp[\mathrm{i}\left(\omega_0-\omega\right)(t-t_1)]. \tag{15}$$

In the following, we consider the case each qubit simultaneously coupled to K reservoirs with Lorentzian spectral densities, and $\boldsymbol{J}(\omega)$ being the sum of spectral densities $J_i(\omega)=\gamma_i\lambda_i^2/\left\{2\pi\left[\left(\omega-\omega_0\right)^2+\lambda_i^2\right]\right\}$ of all the K individual reservoirs, with γ_i the decay rate of the excited state of the qubit and λ_i^{-1} the spectral width of the noise. For simplicity, we assume all reservoirs with identical system–reservoir couplings, i.e., $\gamma_i/\lambda_i=\gamma/\lambda\ \forall i$. Therefore, the analytic expression of time-function $C_{\mathrm{e}}(t)$ can be expressed as

$$C_{\mathrm{e}}(t)=\mathrm{e}^{-\lambda t}\left[\cosh\left(\frac{Wt}{2}\right)+\frac{\lambda}{W}\sinh\left(\frac{Wt}{2}\right)\right], \tag{16}$$

where $W=\sqrt{\lambda^2-2K\gamma\lambda}$. As pointed out in Ref. [56], the parameters λ, γ, and the number of reservoirs K can distinguish the Markovian and non-Markovian regimes. The dynamics of qubit is essentially Markovian under the weak coupling condition $\lambda>2K\gamma$, while it becomes non-Markovian when $\lambda<2K\gamma$. Evidently, the dynamical behavior of the atomic system can be modified by the number of reservoirs K.

Following the procedure in Ref. [57], we could obtain the reduced density matrix of qubit $\rho^{\mathrm{A(B)}}(t)$ in the standard basis $\{|1\rangle,|0\rangle\}$ as

$$\rho^{\mathrm{A(B)}}(t)=\begin{pmatrix}\rho_{11}(0)|C_{\mathrm{e}}(t)|^2 & \rho_{10}(0)C_{\mathrm{e}}(t)\\ \rho_{01}(0)C_{\mathrm{e}}^{*}(t) & \rho_{00}(0)+\rho_{11}(0)\left(1-|C_{\mathrm{e}}(t)|^2\right)\end{pmatrix}. \tag{17}$$

To study the quantum correlation dynamics for two identical qubits, we need the expression of the two-qubit density matrix at time t, which can be constructed from the evolution of single-qubit reduced density matrices Eq. (17) and a standard procedure.[57] Thus, in the standard basis $\{|11\rangle,|10\rangle,|01\rangle,|00\rangle\}$, the diagonal elements of the two-qubit density matrix $\rho^{\mathrm{AB}}(t)$ at time t can be obtained as

$$\begin{aligned}\rho_{11}^{\mathrm{AB}}(t) &= \rho_{11}^{\mathrm{AB}}(0)|C_{\mathrm{e}}(t)|^4,\quad \rho_{22}^{\mathrm{AB}}(t)=|C_{\mathrm{e}}(t)|^2\left[\rho_{22}^{\mathrm{AB}}(0)+\rho_{11}^{\mathrm{AB}}(0)\left(1-|C_{\mathrm{e}}(t)|^2\right)\right],\\ \rho_{33}^{\mathrm{AB}}(t) &= |C_{\mathrm{e}}(t)|^2\left[\rho_{33}^{\mathrm{AB}}(0)+\rho_{11}^{\mathrm{AB}}(0)\left(1-|C_{\mathrm{e}}(t)|^2\right)\right],\quad \rho_{44}^{\mathrm{AB}}(t)=1-\left[\rho_{11}^{\mathrm{AB}}(t)+\rho_{22}^{\mathrm{AB}}(t)+\rho_{33}^{\mathrm{AB}}(t)\right],\end{aligned} \tag{18}$$

and the non-diagonal elements

$$\begin{aligned}\rho_{12}^{\mathrm{AB}}(t) &= \rho_{12}^{\mathrm{AB}}(0)C_{\mathrm{e}}(t)|C_{\mathrm{e}}(t)|^2,\quad \rho_{13}^{\mathrm{AB}}(t)=\rho_{13}^{\mathrm{AB}}(0)C_{\mathrm{e}}(t)|C_{\mathrm{e}}(t)|^2,\\ \rho_{14}^{\mathrm{AB}}(t) &= \rho_{14}^{\mathrm{AB}}(0)[C_{\mathrm{e}}(t)]^2,\quad \rho_{23}^{\mathrm{AB}}(t)=\rho_{23}^{\mathrm{AB}}(0)|C_{\mathrm{e}}(t)|^2,\\ \rho_{24}^{\mathrm{AB}}(t) &= \rho_{24}^{\mathrm{AB}}(0)C_{\mathrm{e}}(t)+\rho_{13}^{\mathrm{AB}}(0)C_{\mathrm{e}}(t)\left(1-|C_{\mathrm{e}}(t)|^2\right),\\ \rho_{34}^{\mathrm{AB}}(t) &= \rho_{34}^{\mathrm{AB}}(0)C_{\mathrm{e}}(t)+\rho_{12}^{\mathrm{AB}}(0)C_{\mathrm{e}}(t)\left(1-|C_{\mathrm{e}}(t)|^2\right),\end{aligned} \tag{19}$$

where $\rho_{ij}^{\mathrm{AB}}(t)=\rho_{ji}^{\mathrm{AB}*}(t)$ with $\rho^{\mathrm{AB}}(t)$ being a hermitian matrix. Equations (18) and (19) clearly describe the time evolution of two qubits for any given initial state. Here we assume that the two qubits are initially in a maximally entangled state, which has the following form:

$$|\Psi(0)\rangle=1/\sqrt{2}\left(|11\rangle+|00\rangle\right). \tag{20}$$

Combining Eqs. (18)–(20), the reduced time-evolving density matrix $\rho^{\mathrm{AB}}(t)$ becomes

$$\rho^{\mathrm{AB}}(t)=\frac{1}{2}\begin{pmatrix}|\upsilon|^2 & 0 & 0 & \upsilon\\ 0 & |\upsilon|-|\upsilon|^2 & 0 & 0\\ 0 & 0 & |\upsilon|-|\upsilon|^2 & 0\\ \upsilon^{*} & 0 & 0 & 2-2|\upsilon|+|\upsilon|^2\end{pmatrix}, \tag{21}$$

with $\upsilon=[C_{\mathrm{e}}(t)]^2$. In the following, we display the dynamic evolution of both two-norm GQD and one-norm GQD for the two-qubit state $\rho^{\mathrm{AB}}(t)$.

4. Environmental effects on the two-norm GQD and one-norm GQD

The dynamical behaviors of the two-norm GQD $D^2(t)$ (red solid line) and the one-norm GQD $D^1(t)$ (blue dot line) are depicted in Fig. 1 for different number of reservoirs K in the weak coupling regime $\gamma=0.4\lambda$. Here, $K=1$ indicates the qubit interacts with one reservoir, the weak system–reservoir coupling regime resulting in the system's Markovian dynamics. In the presence of more than one reservoir, the system's dynamics would becomes non-Markovian. $D^2(t)=D^1(t)=1$ at $\lambda t=0$ implies that there is maximum quantum correlations at the initial time. From Fig. 1(a), we can see that both $D^2(t)$ and $D^1(t)$ decay monotonically with the dimensionless time λt and suffers from a 'sudden death (SD)'. This means that the local environmental noise leads to a decoherence effect on $D^2(t)$ and $D^1(t)$. When the reservoir number K increases to 3, $D^1(t)$ exhibits oscillatory behavior, which can be seen from Fig. 1(b). When K increases further (see Figs. 1(c) and 1(d)), both $D^2(t)$ and $D^1(t)$ become the oscillating functions of time λt. At the same time, the oscillation frequency increases with the reservoir number K. Insets in Figs. 1(c) and 1(d) reflect the non-Markovian behaviors of $D^2(t)$ and $D^1(t)$. The introduction of K can transform the Markovian dynamics to the non-Markovian dynamics. Furthermore, we can know that $D^2(t)$ is always smaller than $D^1(t)$ (except in the case of initial evolutionary time). Additionally, the death phenomenon of $D^2(t)$ emerges earlier compared to $D^1(t)$.

The corresponding dynamic evolutions of the two-norm GQD $D^2(t)$ and the one-norm GQD $D^1(t)$ are presented in Fig. 2 for the strong coupling regime $\gamma=4\lambda$. In this regime, the quantum system can always exhibit the non-Markovian dynamics for any K. In comparison with Fig. 1, both the frequency and amplitude of $D^2(t)$ and $D^1(t)$ are larger with the

same reservoir number K in Fig. 2. That is to say the larger K can enhance the non-Markovianity of the overall environment. However, the survival time of $D^2(t)$ and $D^1(t)$ is just the opposite, because the increase of γ results in the information exchange between qubits and the reservoirs more frequently.

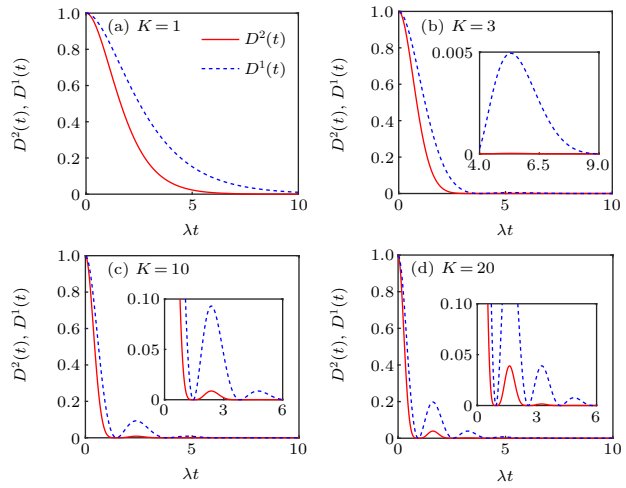


Fig. 1. The two-norm GQD $D^2(t)$ (red solid line) and one-norm GQD $D^1(t)$ (blue dot line) as a function of dimensionless time λt in the weak coupling regime $\gamma = 0.4\lambda$ for $K = 1$ (a), $K = 3$ (b), $K = 10$ (c) and $K = 20$ (d), respectively.

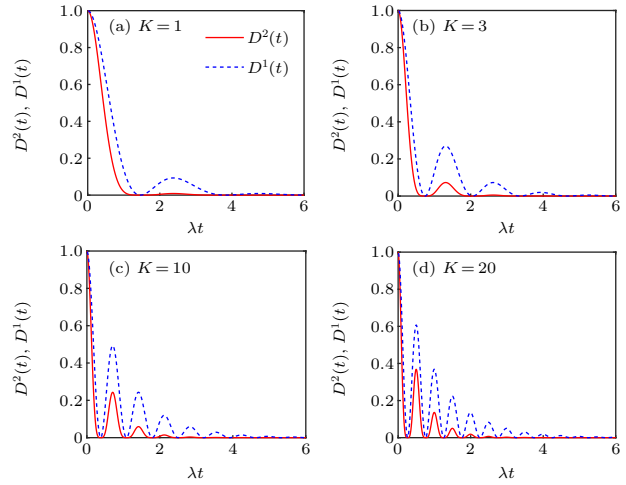


Fig. 2. The two-norm GQD $D^2(t)$ (red solid line) and one-norm GQD $D^1(t)$ (blue dot line) as a function of dimensionless time λt in the strong coupling regime $\gamma = 4\lambda$ for $K = 1$ (a), $K = 3$ (b), $K = 10$ (c) and $K = 20$ (d), respectively.

5. Enhance the GQD with partially collapsing measurements

Quantum coherence plays an important role in quantum information processing, so it is urgent to protect quantum coherence from environmental effects. In recent years, various protection measures have been proposed, such as quantum Zeno effect,[58] decoherence-free subspace,[59] quantum error correction code,[60] and filtering operation.[61] Among which, the partially collapsing measurement method is one of the effective methods to protect the quantum coherence that has received much attention.[62] Partially collapsing measurement consists of quantum weak measurement (WM) and measurement reversal operation (WMR). For a single qubit, quantum weak measurement operation $M_{\rm wk}$ and measurement inversion operation $M_{\rm rev}$ in the standard basis $\{|1\rangle, |0\rangle\}$ can be respectively written as

$$M_{\rm wk} = \begin{pmatrix} \sqrt{1-m} & 0 \\ 0 & 1 \end{pmatrix}, \quad M_{\rm rev} = \begin{pmatrix} 1 & 0 \\ 0 & \sqrt{1-r} \end{pmatrix}. \tag{22}$$

Here m $(0 \le m < 1)$ is the weak measurement strength, and r $(0 \le r < 1)$ is the measurement reversal strength. Obviously, the quantum weak measurement operation can increase the weight of the ground state, while the measurement reversal operation is just the opposite. The effective combination of these two operations can make the quantum state return to the initial state with a certain probability.

Now, performing partially collapsing measurements on two qubits simultaneously, with the initial state being as the form as Eq. (20), we can obtain the final state $\hat{\rho}(t)$

$$\hat{\rho}(t) = \frac{1}{P} \begin{pmatrix} \tilde{\rho}_{11}(t) & 0 & 0 & \tilde{\rho}_{14}(t) \\ 0 & \tilde{\rho}_{22}(t) & 0 & 0 \\ 0 & 0 & \tilde{\rho}_{33}(t) & 0 \\ \tilde{\rho}_{41}(t) & 0 & 0 & \tilde{\rho}_{44}(t) \end{pmatrix} \tag{23}$$

with

$$\begin{aligned} &\tilde{\rho}_{11}(t) = (1-m)^2 |\upsilon|^2, \\ &\tilde{\rho}_{22}(t) = \tilde{\rho}_{33}(t) = (1-m)^2(1-r)|\upsilon|(1-|\upsilon|), \\ &\tilde{\rho}_{44}(t) = (1-r)^2\left[1+(1-m)^2(1-|\upsilon|)^2\right], \\ &\tilde{\rho}_{14}(t) = \tilde{\rho}_{41}^*(t) = (1-m)(1-r)\upsilon, \end{aligned}$$

where $P = \tilde{\rho}_{11}(t) + \tilde{\rho}_{22}(t) + \tilde{\rho}_{33}(t) + \tilde{\rho}_{44}(t)$ is the success probability. In the following, to gain the maximum quantum correction, we will choose the optimal measurement reversals strength $r = 1 - (1-m)|\upsilon|$.

In practice, the quantum state in a complex system, composed of two qubits and the multiple bosonic reservoirs, is affected by the parameter m. There is no initial correlation between the qubits A, B and the environment considered in this paper, but the correlation between qubits A, B and the environment will be redistributed in the course of time evolution. It is well known that the excitation of the system qubits is transferred to that of the environment qubits which causes decoherence, and the flow of information has an effect on quantum geometric discord. Here, Eqs. (21) and (23) respectively describe the reduced density matrix of qubits after tracing the environment without and with the partially collapsing measurements. Comparison of Eqs. (21) and (23) reveals the effect of the partially collapsing measurements on quantum state. The system qubits after the prior weak measurement has moved closer to the $|00\rangle$ state that is less vulnerable to decoherence. A post measurement reversal operation with suitably chosen strength can make the system state close to the initial state. Thus the combination of these two operations will lead to the enhancement of GQD.

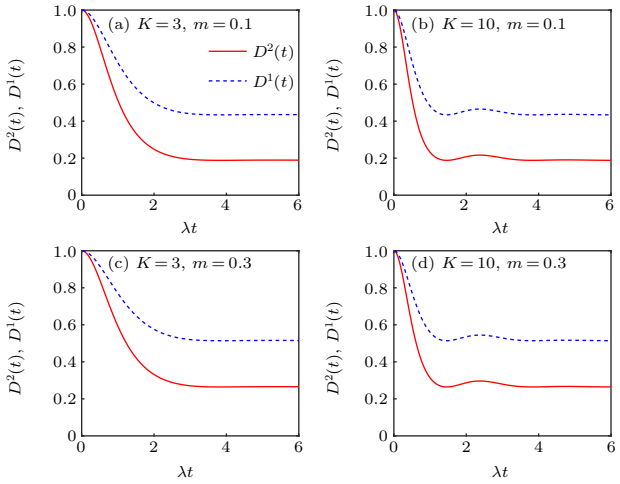


Fig. 3. The dynamic evolutions of two-norm GQD $D^2(t)$ (red solid line) and the one-norm GQD $D^1(t)$ (blue dot line) under partially collapsing measurements with $m = 0.1$ (upper panel) and $m = 0.3$ (lower panel) in the weak coupling regime $\gamma = 0.4\lambda$. The number of reservoirs K is $K = 3$ [(a), (c)] and $K = 10$ [(b), (d)], respectively.

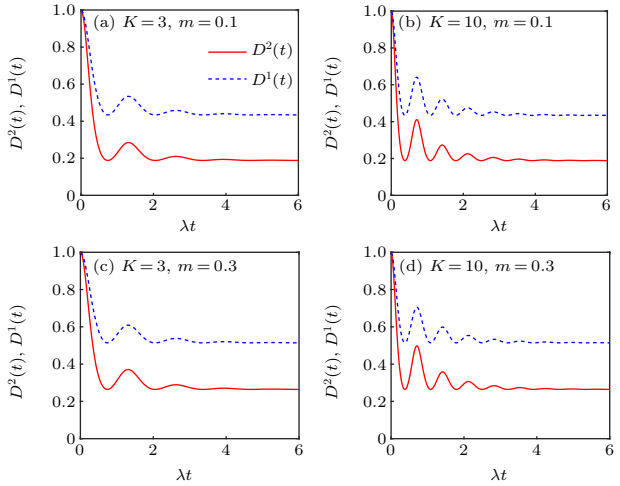


Fig. 4. The dynamic evolutions of two-norm GQD $D^2(t)$ (red solid line) and the one-norm GQD $D^1(t)$ (blue dot line) under partially collapsing measurements with $m = 0.1$ (upper panel) and $m = 0.3$ (lower panel) in the strong coupling regime with $\gamma = 4\lambda$. The number of reservoirs K is $K = 3$ [(a), (c)] and $K = 10$ [(b), (d)], respectively.

The dynamic evolutions of the two-norm GQD $D^2(t)$ (red solid line) and the one-norm GQD $D^1(t)$ (blue dot line) in the presence of partially collapsing measurements are plotted in Fig. 3 for the number of reservoirs $K = 3$ (left panel) and $K = 10$ (right panel), in which Fig. 3 corresponds to the weak coupling regime with $\gamma = 0.4\lambda$. As depicted in Figs. 3(a) and 3(b), for two different number of reservoirs K, after a finite time evolution, $D^2(t)$ and $D^1(t)$ can reach their own stable value with the same weak measurement strength $m = 0.1$. In other words, $D^2(t)$ and $D^1(t)$ can reach the stable value independent of the number of reservoirs K. When $m = 0.3$ (see Figs. 3(c) and 3(d)), their final stable values of $D^2(t)$ and $D^1(t)$ are larger than the case $m = 0.1$. The bigger stable value of $D^2(t)$ and $D^1(t)$ can be obtained when the larger m is given. Moreover, the stable value of $D^2(t)$ is always smaller than $D^1(t)$.

Next, we turn to investigate the effect of this measurements on $D^2(t)$ and $D^1(t)$ in the strong coupling regime $\gamma = 4\lambda$. Choosing the same system parameters as those in Fig. 3, we plot the numerical results for the dependence of $D^2(t)$ and $D^1(t)$ on λt and with different weak measurement strength m in Fig. 4. From these plots we can observe that $D^2(t)$ and $D^1(t)$ achieve their own steady values in a finite time after several non-constant amplitude oscillations. We can find from Figs. 3 and 4 that the final stable values of $D^2(t)$ and $D^1(t)$ are independent of the parameter γ.

6. Conclusion

We use $D^2(t)$ and $D^1(t)$ as a combined tool to investigate the dynamics of quantum correlations in a two-qubit system with each qubit simultaneously interacting with K independent reservoirs of field modes. We study the effects of the number of reservoirs on the dynamics of $D^2(t)$ and $D^1(t)$ in detail. In the weak qubit–reservoirs coupling regimes, $D^2(t)$ and $D^1(t)$ asymptotically decay with the increasing time implying a Markovian dynamics when the number of reservoirs $K = 1$. Then $D^2(t)$ and $D^1(t)$ show non-constant amplitude oscillations when $K = 10$ and 20. The dynamic evolution of $D^2(t)$ and $D^1(t)$ becomes non-monotonic signifying an emergence of the system's non-Markovian dynamics. Increasing K induces an enhancement of memory effects, and causes the transition of the dynamics from Markovian to non-Markovian. In the strong qubit–reservoirs coupling regimes, $D^2(t)$ and $D^1(t)$ exhibit the oscillation behavior for any K. There is an enhancement of the non-Markovianity by increasing the number of reservoirs. In addition, $D^2(t)$ and $D^1(t)$ tend to zero slower in the weak qubit–reservoirs coupling regime than in the strong qubit–reservoirs coupling regime. And $D^2(t)$ is always smaller than $D^1(t)$ except for the initial evolution time. We find that partially collapsing measurements can be used to protect $D^2(t)$ and $D^1(t)$ against the decoherence. When use the partially collapsing measurements, $D^2(t)$ and $D^1(t)$ can reach their own stable values independently of the parameter γ and the number of reservoirs K. The study of partially collapsing measurements is rather significant in the course of quantum information processing.

Acknowledgment

Project supported by the National Natural Science Foundation of China (Grant No. 11772177).

References

[1] Ekert A and Jozsa R 1996 *Rev. Mod. Phys.* **68** 733
[2] Gottesman D and Chuang I L 1999 *Nature* **402** 390
[3] Bennett C H and DiVincenzo D P 2000 *Nature* **404** 247
[4] Takita M, Cross A W, Corcoles A D, Chow J M and Gambetta J M 2017 *Phys. Rev. Lett.* **119** 180501

[5] Bennett C H, Brassard G, Crepeau C, Jozsa R, Peres A and Wootters W K 1993 *Phys. Rev. Lett.* **70** 1895
[6] Ekert A K 1991 *Phys. Rev. Lett.* **67** 661
[7] Dan K, Mor T and Ratsaby G 2012 *Quantum Inf. Comput.* **6** 606
[8] Ollivier H and Zurek W H 2001 *Phys. Rev. Lett.* **88** 017901
[9] Datta A 2009 *Phys. Rev. A* **80** 052304
[10] Li J Q and Liang J Q 2011 *Phys. Lett. A* **375** 1496
[11] Zeng S P, Shi H L, Zhou X, Wang X H, Liu S Y and Hu M L 2019 *Sci. Rep.* **9** 1083
[12] Kon W Y, Krisnanda T, Sengupta P and Paterek T 2019 *Phys. Rev. B* **100** 235103
[13] Meher N, Patoary A S M, Kulkarni G and Jha A K 2020 *J. Opt. Soc. Am B* **37** 1224
[14] Virzì S, Rebufello E, Avella A, Piacentini F, Gramegna M, Berchera I R, Degiovanni I P and Genovese M 2019 *Sci. Rep.* **9** 3030
[15] Chen M C, Zhong H S, Li Y, Wu D, Wang X L, Li L, Liu N L, Lu, C Y and Pan J W 2019 *Sci. Bull.* **64** 580
[16] Cao W, Lu X, Meng X, Sun J, Shen H and Xiao Y 2020 *Phys. Rev. Lett.* **124** 030401
[17] Datta A, Shaji A and Caves C M 2008 *Phys. Rev. Lett.* **100** 050502
[18] Piani M, Horodecki P and Horodecki R 2008 *Phys. Rev. Lett.* **100** 090502
[19] Dakić B, Lipp Y O, Ma X, Ringbauer M, Kropatschek S, Barz S, Paterek T, Vedral V, Zeilinger A, Brukner Č and Walther P 2012 *Nat. Phys.* **8** 666
[20] Brodutch A and Terno D R 2010 *Phys. Rev. A* **81** 062103
[21] De Chiara G and Sanpera A 2018 *Rep. Prog. Phys.* **81** 074002
[22] Luo S 2008 *Phys. Rev. A* **77** 42303
[23] Ali M, Rau A R P and Alber G 2010 *Phys. Rev. A* **81** 82
[24] Knill E and Laflamme R 1998 *Phys. Rev. Lett.* **81** 5672
[25] Horodecki M, Horodecki P and Horodecki R 2005 *Phys. Rev. A* **71** 062307
[26] Luo S and Fu S 2011 *Phys. Rev. Lett.* **106** 120401
[27] Dakic B, Vedral V and Brukner C 2010 *Phys. Rev. Lett.* **105** 190502
[28] Luo S 2008 *Phys. Rev. A* **77** 042303
[29] Rulli C C and Sarandy M S 2011 *Phys. Rev. A* **84** 042109
[30] Hu X, Fan H, Zhou D L and Liu W M 2013 *Phys. Rev. A* **87** 032340
[31] Tufarelli T, Girolami D, Vasile R, Bose S and Adesso G 2012 *Phys. Rev. A* **86** 052326
[32] Piani M 2012 *Phys. Rev. A* **86** 034101
[33] Paula F M, Oliveira T R D and Sarandy M S 2013 *Phys. Rev. A* **87** 064101
[34] Mohamed A B A 2012 *Ann. Phys.* **327** 3130
[35] Zhang G F, Ji A L, Fan H and Liu W M 2012 *Ann. Phys.* **327** 2074
[36] Zhang G F, Fan H, Ji A L and Liu W M 2012 *Eur. Phys. J. D* **66** 34
[37] Ramzan M 2013 *Quantum Inf. Process.* **12** 2721
[38] Hu M L and Lian H L 2015 *Ann. Phys.* **362** 795
[39] Bai X M, Wang N, Li J Q and Liang J Q 2016 *Quantum Inf. Process.* **15** 2771
[40] Mohamed A B A and Metwally N 2019 *Quantum Inf. Process.* **18** 79
[41] Orthey Jr A C and Angelo R M 2019 *Phys. Rev. A* **100** 042110
[42] Bemani F, Roknizadeh R, Motazedifard A, Naderi M H and Vitali D 2019 *Phys. Rev. A* **99** 063814
[43] Kenfack L T, Tchoffo M, Javed M and Fai L C 2020 *Quantum Inf. Process.* **19** 107
[44] Mohamed A B A, Hessian H A and Eleuch H 2020 *Chaos Soliton Fract.* **135** 109773
[45] Vimal V K and Subrahmanyam V 2020 *Phys. Rev. A* **102** 012406
[46] Ban M 2020 *Quantum Inf. Process* **19** 46
[47] Pourkarimi M R and Haddadi S 2020 *Laser Phys. Lett.* **17** 025206
[48] Li X X, Yin H D, Li D X and Shao X Q 2020 *Phys. Rev. A* **101** 012329
[49] Apollaro T J G, Lorenzo S, DiFranco C, Plastina F and Paternostro M 2014 *Phys. Rev. A* **90** 012310
[50] Chan C K, Lin G D, Yelin S F and Lukin M D 2014 *Phys. Rev. A* **89** 042117
[51] Hanson R, Dobrovitski V V, Feiguin A E, Gywat O and Awschalom D D 2008 *Science* **320** 352
[52] Altintas F 2010 *Opt. Commun* **283** 5264
[53] Montealegre J D, Paula F M, Saguia A and Sarandy M S 2013 *Phys. Rev. A* **87** 042115
[54] Nakano T, Piani M and Adesso G 2013 *Phys. Rev. A* **88** 012117
[55] Ciccarello F, Tufarelli T and Giovannetti V 2014 *New. J. Phys.* **16** 013038
[56] Man Z X, An N B and Xia Y J 2014 *Phys. Rev. A* **90** 062104
[57] Bellomo B, Franco R L and Compagno G 2007 *Phys. Rev. Lett.* **99** 160502
[58] Facchi P, Lidar D A and Pascazio S 2004 *Phys. Rev. A* **69** 032314
[59] Lidar D A, Chuang I and Whaley K B 1998 *Phys. Rev. Lett.* **81** 2594
[60] Knill E and Laflamme R 1997 *Phys. Rev. A* **55** 900
[61] Huang A J, Shi J D, Wang D and Ye L 2017 *Quantum Inf. Process* **16** 46
[62] Ding Z Y, He J and Ye L 2016 *Ann. Phys.* **377** 96